Predicting the Response of an All-Elastomer In-Plane MEMS Tactile Sensor

K. M. Kalayeh*, A. Charalambides** , S. Bergbreiter**, and P. G. Charalambides*

* The University of Maryland, Baltimore County, Baltimore, MD 21250
** ME Department, Institute of System Research,
The University of Maryland, College Park, MD 20742

ABSTRACT

A large deformation mechanics model is employed in predicting capacitance changes in an all-elastomer capacitive tactile sensor, and the predictive model is experimentally validated. The compressive model predicts a non-linear relationship between the contact normal force and resulting capacitance change due to changes in electrode gap and electrode layer thickness. Broad parametric studies demonstrate that higher sensing capabilities can be achieved when using sensors made of softer materials and smaller electrode gaps. Sensors are fabricated using a reusable silicon mold and experimental results are compared to predictions from the capacitance model. Calibrated capacitance-force model predictions are shown to be in remarkable agreement with experimental measurements. A fringe effects term included in the capacitance model highlights the limitations of the parallel plate model especially for sensors with large electrode layer gaps.

Keywords: capacitive tactile sensor, experimental validation, microfabrication, non-linear predictive model, parametric studies

1 INTRODUCTION

The developments of advanced technologies in robotic grasping, motion of prosthetics, and robot assisted biomedical surgery require "real-time" knowledge of applied forces and their locations. In response, in recent years, tactile sensor technologies received increased attention [1, 2] aimed at addressing both fabrication challenges as well as performance goals. Recent developments in microfabrication technologies have enabled the development of Micro-Electro-Mechanical Systems (MEMS) tactile sensors that have shown to have increased spatial resolution while manufactured at relatively low cost and large quantities [3, 4]. Since these sensors usually need to be mounted on curved surfaces, it is critical that they are flexible to bend as well as stretchable [5]. Thus, soft polymer-based materials such as polyimide (PI), or polydimethlysiloxane (PDMS) are used as the substrate phase for flexible MEMS sensors [3, 4]. Among many sensors, capacitive tactile sensors

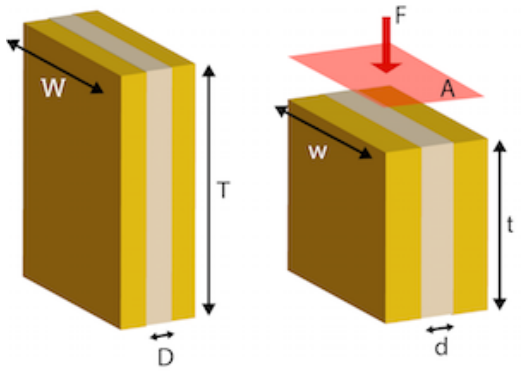

Figure 1: An applied pressure compresses and expands the all-elastomer sensor through Poisson's effect, resulting in a decreased capacitance across the electrodes. The electrodes (color: gold) are sandwiched by the dielectric layer (color: beige).

are known to be characterized by better spatial resolution and higher sensitivity.

2 SENSOR MODEL

In-plane capacitive tactile sensor has been designed and fabricated in [3, 6]. The schematic of the designed sensor is shown in Fig. 1. A rectangular sensor geometry that undergoes a uniform compressive stress will compress in the direction of the applied force and expand perpendicularly to the applied force as governed by Poisson's ratio. Given the material properties, the deformation (and ultimately capacitance) can be related to the force and applied pressure. This physical phenomenon can be measured by placing compliant electrodes on either end of the deformed material, so that the deformation is correlated to a change in capacitance across the electrodes.

2.1 The Large Deformation Layer Compression Model

The working principle of the designed sensor is shown in Fig. 2(a). As shown, conductive electrodes of initial thickness T are embedded in a thin elastomeric layer of thickness H. The electrodes are separated by initial gap D. Upon contact the top surface of the sensor may compress by a uniform deformation U. Thus, the initial

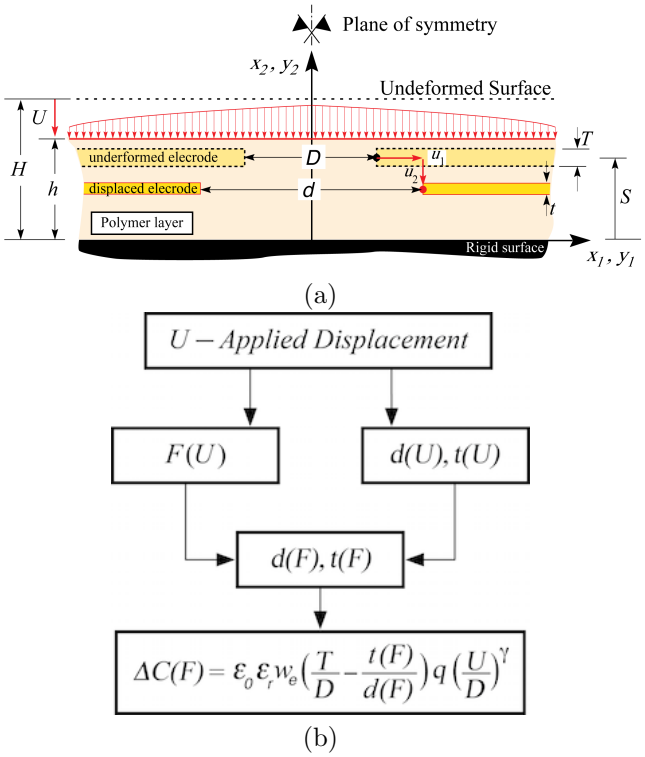

Figure 2: (a) A cross-sectional view of the sensor designed and modeled in this study. (b) A flow chart indicating the process used to establish the relationship between the sensor capacitance $C(F)$ and the applied contact force F. The constants q and γ are determined through model calibration studies.

layer thickness H decreases to h, while the electrode gap D increases to d, and the electrode thickness T decreases to t. Consistent with the flowchart shown in Fig. 2 (b), the change in capacitance can be related to the applied force using the large deformation and force-capacitance model developed in [6, 7] which utilizes the electrode gap and thickness changes during contact.

The schematic of the boundary value problem (BVP) solved in [7] is shown in Fig. 3. The displacement of a point Q shown in the above figure is given by it's displacement along both the 1 and 2 axes,

$$u_1(x_1, x_2) = y_1 - x_1 = x_1(f(x_2) - 1), \tag{1a}$$
$$u_2(x_2) = y_2 - x_2 = g(x_2) - x_2, \tag{1b}$$

where $f(x_2)$ and $g(x_2)$ are found out to be,

$$f(x_2) = \cos(\alpha x_2) + \tan(\alpha H)\sin(\alpha x_2), \tag{2}$$

$$g(x_2) = \frac{\cos(\alpha H)}{\alpha}\left(\log\frac{1+\sin(\alpha H)}{1-\sin(\alpha H)} - \log\frac{1+(\tan(\alpha H)-\tan(\frac{\alpha x_2}{2}))\cos(\alpha H)}{1-(\tan(\alpha H)-\tan(\frac{\alpha x_2}{2}))\cos(\alpha H)}\right). \tag{3}$$

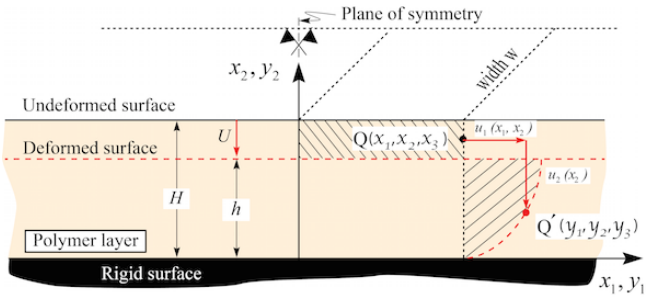

Figure 3: A schematic showing the infinitely long soft polymeric layer subjected to uniform displacement U along its top surface.

In the above equations, H is the initial layer height and αH is a constant that depends on the relative layer compression U/H. The value of αH can be determined by enforcing $g(x_2 = H) = h$, with h as the deformed layer thickness, i.e., $h = H - U$. A complete lookup table of αH values computed by solving the nonlinear equation $g(H) = h$ is given in [7].

Furthermore, based on the above model, the non-trivial Cauchy stress components can be expressed as follows,

$$\sigma_{11} = -P + C_1(f^2 + (x_1 f')^2) + C_2 g'^2, \tag{4a}$$
$$\sigma_{12} = (C_1 - C_2) x_1 f' g', \tag{4b}$$
$$\sigma_{22} = -P + C_1 g'^2 + C_2(f^2 + x_1^2 f'^2), \tag{4c}$$

in which C_1 and C_2 are Mooney-Rivlin (M-R) material constants, and $P(x_1, x_2)$ is the pressure and is given by,

$$P = C_2 x_1^2 f'^2 + \frac{(C_1 - C_2)}{2} A x_1^2 f^2 + \frac{(C_1 + C_2)}{2}\frac{1}{f^2} + C_2 f^2 + \Pi, \tag{5}$$

with the constant Π determined with the aid of global equilibrium as discussed in [7]. Analytical and finite element (FE) results were shown to agree in [7] over a broad range of layer compression with the most severe case reported to be $U/H = 0.4$, corresponding to 40 % layer thinning.

2.2 Sensor Contact Force

With the aid of the large deformation model developed in [7], the applied force over undeformed contact area $2L_c \times w_c$ can be expressed as,

$$F = 2 w_c L_c \lambda \left(-\frac{C_1 - C_2}{6} A L^2 \lambda^2 + \frac{C_1 - C_2}{2}\frac{1}{\lambda^2} - \Pi\right), \tag{6}$$

where $\lambda = f(x_2 = H)$ is the principal stretch ratio for material points on the top surface of the polymer layer, and A and Π are constants determined through boundary and global equilibrium conditions and depend on the

layer compression level U/H. The constant A is negative and is given as $A = -\alpha^2$, where α is obtained by solving a non-linear equation resulting from the geometric condition $g(x_2 = H) = h$.

As discussed in detail in [6, 7], the constant Π is calculated by enforcing the global equilibrium in the long layer direction. In doing so, the calibration factors ζ and m are introduced to align the model developed in [7], which assumes infinitely long layer (Fig. 3), with the actual fabricated sensors with finite length. The latter constants are determined through model comparison to experiments.

2.3 Sensor Change in Capacitance

As discussed in [6], an enhanced capacitance model that accounts for both the parallel plate as well as the fringe electric field effects is developed. Based on the proposed model, the change in capacitance, ΔC, can be expressed as follows,

$$\Delta C = C_0 - C = \varepsilon_0 \varepsilon_r w_e \Big(\frac{T}{D} - \frac{t}{d}\Big) q \Big(\frac{U}{D}\Big)^{\gamma}, \tag{7}$$

where the $q(U/D)^{\gamma}$ term is introduced as a modification to the parallel plate capacitance change term constituting the remainder of Eq. (7). The parameters q and γ are obtained through model comparison to experiments. The current electrode gap, d, can be obtained using the large deformation model developed in [7]. The current electrode thickness, on the other hand, is obtained using an empirical expression that accounts for the heterogeneity between the electrodes and the dielectric layer. Based on the relevant finite element studies, a minimum t_{min} is used as an asymptotic value for the maximum electrode layer thinning. Thus, the current thickness t takes the following form,

$$t = t_{min} + (T - t_{min}) e^{-n \frac{U}{H}}, \tag{8}$$

where n is a constant controlling the electrode thinning rate with respect to the layer compression U/H which depends on the electrode gap D. The values of n and t_{min} are reported in Table 1 for all 3 different sensors considered in this study.

3 Experimental Methods

In order to validate the above sensor model , tactile sensors are fabricated using a variation on the micromolding process first reported in [3]. The detail of microfabrication process can be found in [6].

The total thickness of the fabricated sensors was $H = 950$ µm while the dielectric layer width was $w_d = 3{,}500$ µm. Electrode layers of initial thickness $T = 100$ µm were placed at $S = 550$ µm from the bottom sensor surface. Sensors with electrode gaps of 20, 50, and 100 µm were fabricated. Material testing

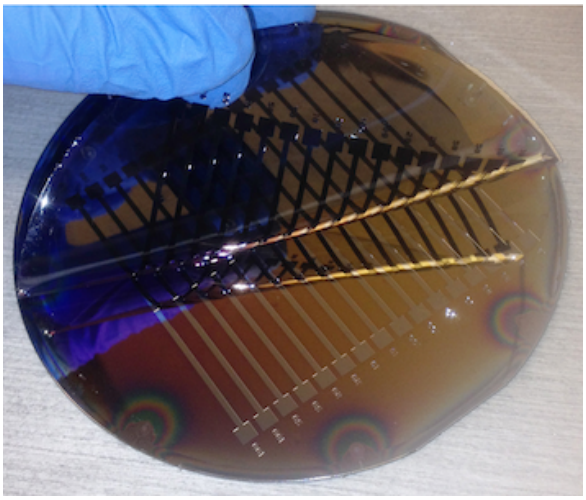

(a)

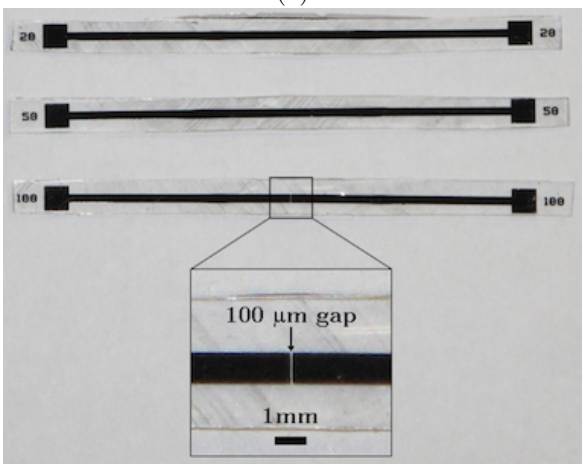

(b)

Figure 4: (a) Peeling of the fabricated sensors from silicon mold, (b) fabricated sensors for 3 different geometries considered in this study.

of these tactile sensors yielded a Modulus of Elasticity $E_d = 1.2$ MPa, for the polymer dielectric layer and that of the composite elastomeric electrode to be $E_e = 2.1$ MPa. The fabricated sensors are shown in Fig. 4.

4 Results

A displacement was applied normal to the electrode gap for three sensors with initial gaps, 20 µm, 50 µm, and 100 µm, to assess each sensor's performance. The relationship of the applied displacement to the measured capacitance was recorded. The model was then used to obtain the force capacitance change curves.

4.1 Capacitance and Force Results

The model uses the sensor geometry variables consistent with fabricated sensors in Sec 3. Model dielectric

Table 1: Model parameters for three different sensor geometries considered in this study.

$D(\mu m)$	ζ	m	t_{min}/T	n	q	γ
20	20	1	0.7	25	1.85	-0.4
50	20	1	0.7	10	2.65	-0.3
100	20	1	0.7	5	0.65	-0.3

constants of $\varepsilon_0 = 8.8541$ pF/m and $\varepsilon_r = 2.4$ are consistent with reported values for Sylgard 184 PDMS.

Model calibration factors, i.e., ζ, m, q, γ are obtained through a best-fit optimization process as discussed in detail in [6]. These parameters are reported in Table 1 for all three sensor geometries considered in this study.

The model predictions for the above optimal calibration factors, q, γ, plotted along with the experimental data is shown in Fig. 5 (Model 1). Furthermore, for comparison purposes, the results obtained using the parallel plate model alone, without fringe field effects are also shown in the same figure (Model 2; dashed lines).

Exceptional agreement is shown to exist between the analytical model (Model 1, with fringe field effects) predictions and the related experimental data. It is noteworthy that the non-linear model developed herein captures the sensor response over the entire applied force envelope. These findings suggest that the current non-linear sensor capacitance model represents a dramatic improvement over existing linear models [3] and that it can be used to predict the sensor response over its entire sensing range.

Broad parametric study were also carried out in [6], which can be used to enhance the performance of these sensors.

5 Conclusions

A predictive non-linear capacitance change model has been developed for tactile capacitance sensors subjected to pressure loading. This new model expands existing linear model capabilities and can be used to predict the sensor response over its entire sensing range. The model incorporates the non-linear deformation mechanics for a soft elastomeric layer subjected to uniform compressive displacement condition. The model was properly adjusted to incorporate the finite contact probe effects through a rigorous shear stress integration technique. The capacitance change model was embedded into an optimization algorithm aimed at identifying model parameters that resulted in best fit model predictions with reported experimental data for three self-similar sensor systems. The calibrated model predictions were shown to be in excellent agreement with the experimental results over the entire applied force range for all three sensor tested.

The model capabilities were further explored by conducting broad parametric studies aimed at investigating

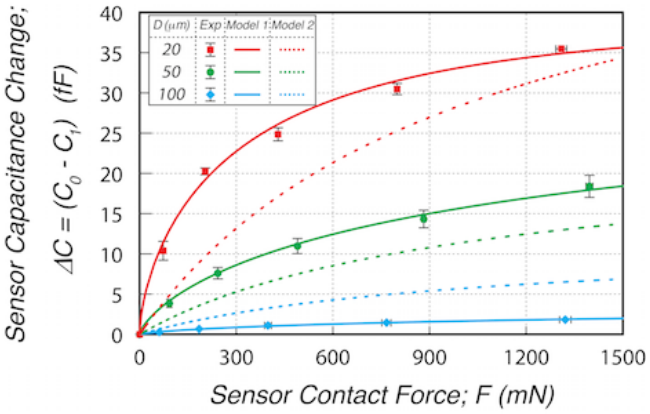

Figure 5: Change in capacitance as a function of applied normal force for flat plate capacitors of various dielectric gaps.

the effects of layer modulus, electrode layer properties, electrode layer location and thickness as well as the effects of electrode layer gap. The outcomes suggest that the current capacitance model has broad predictive capabilities that may assist in the optimal design of related all-elastomer MEMS tactile sensors.

REFERENCES

[1] "Syntouch," http://www.syntouchllc.com/, accessed: 12/22/2015.

[2] "Bionx medical technologies, inc." http://www.bionxmed.com/, accessed: 12/22/2015.

[3] A. Charalambides and S. Bergbreiter, "All-elastomer in-plane MEMS capacitive tactile sensor for normal force detection," in *2013 IEEE Sensors*, 2013, pp. 1–4.

[4] A. Charalambides and S. Bergbeiter, "A novel all-elastomer MEMS tactile sensor for high dynamic range shear and normal force sensing," *Journal of Micromechanics and Microengineering*, vol. 25, no. 9, p. 095009, 2015.

[5] G. Liang, Y. Wang, D. Mei, K. Xi, and Z. Chen, "A modified analytical model to study the sensing performance of a flexible capacitive tactile sensor array," *Journal of Micromechanics and Microengineering*, pp. 1–14, 2015.

[6] K. M. Kalayeh, A. G. Charalambides, S. Bergbreiter, and P. G. Charalambides, "Model and experimental validation of an all-elastomer in-plane capacitive tactile sensor," *Submitted to IEEE, Sensors Journal*, 2015.

[7] K. M. Kalayeh and P. G. Charalambides, "Large deformation mechanics of a soft elastomeric layer under compressive loading for a MEMS tactile sensor application," *International Journal of Non-Linear Mechanics*, vol. 76, pp. 120–134, 2015.